© 2018. Published by The Company of Biologists Ltd | Development (2018) 145, dev164830. doi:10.1242/dev.164830

RESEARCH ARTICLE

Enpp1 inhibits ectopic joint calcification and maintains articular chondrocytes by repressing hedgehog signaling

Yunyun Jin[1,2], Qian Cong[1], Jelena Gvozdenovic-Jeremic[3], Jiajie Hu[1], Yiqun Zhang[1], Robert Terkeltaub[4] and Yingzi Yang[1,*]

ABSTRACT

The differentiated phenotype of articular chondrocytes of synovial joints needs to be maintained throughout life. Disruption of the articular cartilage, frequently associated with chondrocyte hypertrophy and calcification, is a central feature in osteoarthritis (OA). However, the molecular mechanisms whereby phenotypes of articular chondrocytes are maintained and pathological calcification is inhibited remain poorly understood. Recently, the ecto-enzyme Enpp1, a suppressor of pathological calcification, was reported to be decreased in joint cartilage with OA in both human and mouse, and *Enpp1* deficiency causes joint calcification. Here, we found that hedgehog (Hh) signaling activation contributes to ectopic joint calcification in the *Enpp1*$^{-/-}$ mice. In the *Enpp1*$^{-/-}$ joints, Hh signaling was upregulated. Further activation of Hh signaling by removing the patched 1 gene in the *Enpp1*$^{-/-}$ mice enhanced ectopic joint calcification, whereas removing *Gli2* partially rescued the ectopic calcification phenotype. In addition, reduction of $G\alpha_s$ in the *Enpp1*$^{-/-}$ mice enhanced joint calcification, suggesting that Enpp1 inhibits Hh signaling and chondrocyte hypertrophy by activating $G\alpha_s$-PKA signaling. Our findings provide new insights into the mechanisms underlying *Enpp1* regulation of joint integrity.

KEY WORDS: Enpp1, Hedgehog signaling, *Gnas*, Osteoarthritis, Ectopic calcification, Mouse

INTRODUCTION

The joint connects neighboring skeletal elements together as a functional unit. The joint cartilage protects the underlying bone from excessive mechanical load, which is distributed across the entire joint surface. The healthy synovial joint is composed of articular cartilage and other joint tissues such as synovial membrane and joint ligaments (Lories and Luyten, 2011). In the healthy joint, the matrix of articular cartilage maintains a relatively low turnover rate and chondrocytes exhibit low proliferation rates, without hypertrophy or terminal differentiation (Dreier, 2010).

The integrity of the complex joint structures has to be maintained throughout life; its disruption causes arthritis, a joint disease that affects >50% of people over the age of 65 and is among the leading causes of disability throughout the world (Guilak, 2011). Osteoarthritis (OA) is the most common type of arthritis (Arai et al., 2004). It is primarily characterized by cartilage breakdown, which is associated with new bone formation at the joint margins (osteophytosis), subchondral bone sclerosis, variable degrees of mild synovitis and thickening of the joint capsule (Sellam and Berenbaum, 2010). Articular cartilage loss is the first sign of OA; the breakdown of cartilage extracellular matrix leads to an early and high incidence of OA (Heinegård and Saxne, 2011). In the osteoarthritic joint, there is ectopic chondrocyte hypertrophy evidenced by the expression of collagen 10a1 (*Col10*, also known as *Col10a1*) and matrix metalloproteinase 13 (*Mmp13*) (Kamekura et al., 2006; Neuhold et al., 2001) in articular cartilage, and these ectopic hypertrophic chondrocytes form calcified cartilage zones (Tchetina, 2011). However, despite detailed histological characterization of OA, the underlying molecular mechanisms whereby articular cartilage degeneration is initiated and advanced, leading to OA, remain poorly understood. This has severely hampered development of pharmacological agents that can prevent or reduce the articular cartilage degeneration and ectopic calcification associated with OA. Multiple risk factors such as hormones, age and levels of calcium (Ca^{2+}), phosphate (P_i) and pyrophosphate (PP_i) in the blood have been found to contribute to the onset and progression of OA. As OA heritability has been suggested to be 50% or more, genetic susceptibility contributes significantly (Spector and MacGregor, 2004; Valdes et al., 2008).

Ectonucleotide pyrophosphatase/phosphodiesterase 1 (Enpp1) is an ecto-enzyme that converts ATP to AMP and PP_i outside of cells. Enpp1 plays an essential role in phosphate homeostasis (Goding et al., 2003). *Enpp1* has been found to be expressed in various cells, including chondrocytes and osteoblasts (Goding et al., 1998), and Enpp1 protein has been detected in articular cartilage in both human and mouse joints (Bertrand et al., 2012). Enpp1 inhibits hydroxyapatite formation by generating PP_i, and thereby inhibits soft tissue calcification (Stefan et al., 2005). In humans, loss-of-function *ENPP1* mutations cause generalized arterial calcification of infancy (GACI) (Ruf et al., 2005; Rutsch et al., 2003) or pseudoxanthoma elasticum (Nitschke and Rutsch, 2012). Enpp1 also represents an important genetic susceptibility factor in OA of the hand, which is the third most common OA, after knee OA and hip OA. A family-based association study showed that genetic variation at the *ENPP1* locus is involved in the etiology of hand OA (Gabay and Gabay, 2013). In mice, loss of function of *Enpp1* results in ectopic calcification of articular cartilage, the joint capsule and certain tendons (Babij et al., 2009; Harmey et al., 2004; Zhang et al., 2016). *Enpp1*$^{-/-}$ mice also exhibit OA-like changes (Bertrand et al., 2012).

Hedgehog (Hh) signaling plays an essential and pivotal role in the regulation of chondrocyte proliferation and hypertrophy during endochondral bone development, in which Indian hedgehog is

[1]Department of Developmental Biology, Harvard School of Dental Medicine, Harvard Stem Cell Institute, Boston, MA 02115, USA. [2]Shanghai Key Laboratory of Regulatory Biology, Institute of Biomedical Sciences and School of Life Sciences, East China Normal University, Shanghai 200241, China. [3]Genetic Disease Research Branch, National Human Genome Research Institute, Bethesda, MD 20892, USA. [4]Department of Medicine, Veterans Affairs Healthcare System, University of California San Diego, 111K, 3350 La Jolla Village Dr., San Diego, CA 92161, USA.

*Author for correspondence (yingzi_yang@hsdm.harvard.edu)

Y.Y., 0000-0003-3933-887X

Received 21 February 2018; Accepted 12 July 2018

Development (2018) 145, dev164830. doi:10.1242/dev.164830

expressed in prehypertrophic and early hypertrophic chondrocytes (Long et al., 2001; Mak et al., 2008b; St-Jacques et al., 1999; Vortkamp et al., 1996). We have shown previously that Hh signaling activation promotes chondrocyte hypertrophy in articular cartilage, and has also been found in human OA (Lin et al., 2009; Mak et al., 2008b). Blockade of Hh signaling can reduce the severity of OA in mice (Lin et al., 2009). We have also found that $G\alpha_s$ inhibits Hh signaling (Regard et al., 2013). In addition, loss of *Gnas*, which encodes $G\alpha_s$, leads to premature chondrocyte hypertrophy (Bastepe et al., 2004). As ATP and its derived products, such as adenosine, which are generated by Enpp1, can signal through G-protein-coupled receptors (GPCR) that can be coupled to $G\alpha_i$ or $G\alpha_s$, Enpp1 may inhibit joint calcification by inhibiting Hh signaling through reducing $G\alpha_i$ signaling and/or upregulating $G\alpha_s$ signaling. To test this hypothesis, we have determined whether Hh signaling is altered in the *Enpp1*$^{-/-}$ joint. We found ectopic upregulation of Hh signaling activity in the articular cartilage of the *Enpp1*$^{-/-}$ mice. Activation of Hh signaling by removing one copy of patched 1 (*Ptch1*), or reduction of Hh signaling by removing one copy of *Gli2*, led to enhanced or reduced ectopic joint calcification in the *Enpp1*$^{-/-}$ mice, respectively. In addition, heterozygous loss of *Gnas* function also enhanced the joint calcification phenotypes of the *Enpp1*$^{-/-}$ mice. Our work suggests that, apart from regulating ATP, PP_i and P_i homeostasis, *Enpp1* deficiency may also cause OA by promoting calcification via activation of the Hh signaling pathway.

RESULTS

Loss of *Enpp1* alters cell differentiation in joints

The *Enpp1*$^{-/-}$ mice developed stiffened joints at ∼4 weeks of age on a standard rodent diet, with progressively mineralized articular cartilage detected from 9 weeks of age (Bertrand et al., 2012; Li et al., 2013; Zhang et al., 2016). To test whether mineralization of the articular cartilage is caused simply by deposition of hydroxyapatite on the articular surfaces, or whether there is loss of articular chondrocyte differentiation and ectopic chondrocyte hypertrophy associated with OA in the joints of the *Enpp1*$^{-/-}$ mice, we first examined gene expression by quantitative real time PCR (qRT-PCR) in the metacarpophalangeal joints of the *Enpp1*$^{-/-}$ and wild-type (WT) control mice at 1 month of age, when there is no joint mineralization (Zhang et al., 2016) (Fig. 1A). In this study, the phalangeal joints between the metacarpal bone and the proximal phalanx of digit three were used for analysis, unless otherwise indicated in the text. The joint tissue was a mixture of cartilage, tendon and synovium. Normal articular chondrocytes strongly express *Col2* (also known as *Col2a1*), aggrecan (*Acan*) and *Sox9*, but not *Col10*, a marker for hypertrophic chondrocytes. In the joints of the *Enpp1*$^{-/-}$ mice, we found that, whereas *Col2*, *Acan* and *Sox9* expression was reduced, *Col10* expression was significantly upregulated. To further examine whether there was hypertrophic chondrocyte differentiation in the articular cartilage of the *Enpp1*$^{-/-}$ mice, we examined the presence of hypertrophic chondrocyte cells using the osterix (*Osx*, also known as *Sp7*) promoter-driven GFP-fused cre recombinase (*OsxGFPcre*) mouse line (Rodda and McMahon, 2006). *Osx* is expressed in hypertropic chondrocytes and is an early marker of committed osteoblast cells (Nakashima et al., 2002). To detect whether *Osx* was ectopically expressed in the phalangeal joint, we generated *OsxGFPcre; Enpp1*$^{-/-}$ mice. The GFP^+ cells should be either hypertrophic chondrocytes or osteoblasts, which express *Osx*. Whereas the control WT *OsxGFPcre* mice had almost no GFP^+ cells in the joint, the number of GFP^+ cells increased ∼20-fold in the articular cartilage and in the joint capsule of the metacarpophalangeal joint of the 4-month-old *Enpp1*$^{-/-}$ mice (Fig. S1A-1A″), in which joint mineralization started at ∼8-9 weeks of age (Hajjawi et al., 2014; Zhang et al., 2016). In addition, we performed immunofluorescent staining of Osx and Sox9 in sections of the 1-month-old WT and *Enpp1*$^{-/-}$ metacarpophalangeal joints. Osx expression was detected in the articular cartilage of the metacarpophalangeal joints of the *Enpp1*$^{-/-}$ mice, but not in that of the WT mice (Fig. 1B-C′). Conversely, Sox9 expression was reduced the *Enpp1*$^{-/-}$ mice compared with the WT control (Fig. 1D-E′). These results indicate that in addition to deposition of hydroxyapatite crystals, the *Enpp1*$^{-/-}$ mice formed ectopic hypertrophic chondrocytes and/or osteoblasts in the articular cartilage and joint capsule.

To further confirm that there was ectopic chondrocyte and/or osteoblast differentiation in the joints of the *Enpp1*$^{-/-}$ mice, we examined expression of other hypertrophic and osteoblast cell markers. We performed *in situ* hybridization (ISH) using postnatal day (P) 2 *Enpp1*$^{-/-}$ forelimb joints and found ectopic expression of collagen1a1 (*Col1a1*) in the articular cartilage of the *Enpp1*$^{-/-}$ mice and increased *Col1a1* expression in the joint capsule (Fig. 1F,F′). Furthermore, using immunofluorescent staining, we found that expression of Mmp13 and osteopontin (Opn, also known as Spp1) were both upregulated in the articular cartilage in the metacarpophalangeal joints of the P2 and 1-month-old *Enpp1*$^{-/-}$ mice, respectively (Fig. 1G,G″ and H-I″). Taken together, these results indicate that in the phalangeal joints of the *Enpp1*$^{-/-}$ mice, there is ectopic chondrocyte hypertrophy and osteoblastic differentiation before ectopic mineralization could be detected.

Loss of *Enpp1* leads to upregulation of Hh signaling in development

Previous studies have demonstrated that Hh signaling promotes chondrocyte hypertrophy and osteoblast differentiation (Lin et al., 2009; Mak et al., 2006; Regard et al., 2013). We hypothesized that Enpp1 may inhibit chondrocyte hypertrophy and/or osteoblast differentiation in the joint by inhibiting Hh signaling. Loss of *Enpp1* may have resulted in activated Hh signaling, causing ectopic calcification. To test this hypothesis, we first examined the expression of the Hh target genes *Gli1* (Bai et al., 2002), *Hhip* (Chuang and McMahon, 1999) and *Ptch1* (Goodrich et al., 1996) in embryonic day (E) 15.5 forelimbs by whole-mount *in situ* hybridization (WISH). *Gli1*, *Hhip* and *Ptch1* expression were all upregulated in the forelimbs of the E15.5 *Enpp1*$^{-/-}$ embryos compared with the WT controls (Fig. 2A-D, Fig. S1B,B′). However, we did not detect obvious ectopic expression of Hh target genes outside their normal expression domains in the *Enpp1*$^{-/-}$ embryos. Upregulation of Hh target gene expression in the forelimbs was further confirmed by qRT-PCR analysis of the E15.5 *Enpp1*$^{-/-}$ and WT embryos (Fig. 2E). In addition, chondrocyte hypertrophy and/or osteogenic differentiation in the forelimbs was increased as shown by qRT-PCR analysis of the E15.5 Enpp1$^{-/-}$ and WT embryos (Fig. 2F). These results show that, early in skeletal formation during embryonic development, Hh signaling is already upregulated in the *Enpp1*$^{-/-}$ limbs.

As ectopic mineralization in the *Enpp1*$^{-/-}$ mice occurs 9 weeks after birth (Zhang et al., 2016), we asked whether ectopic Hh signaling activation in the joint of the *Enpp1*$^{-/-}$ mutants could be detected before ectopic mineralization. We dissected the limbs from the P2 *Enpp1*$^{-/-}$ and WT mice, and gene expression was examined by qRT-PCR. Hh target gene (*Gli1*, *Hhip* and *Ptch1*) expression was increased in the *Enpp1*$^{-/-}$ mutant (Fig. 3A). Chondrocyte hypertrophy and/or osteogenic differentiation was also increased in the *Enpp1*$^{-/-}$ mutant, as shown by increased expression of osteoblast

Development (2018) 145, dev164830. doi:10.1242/dev.164830

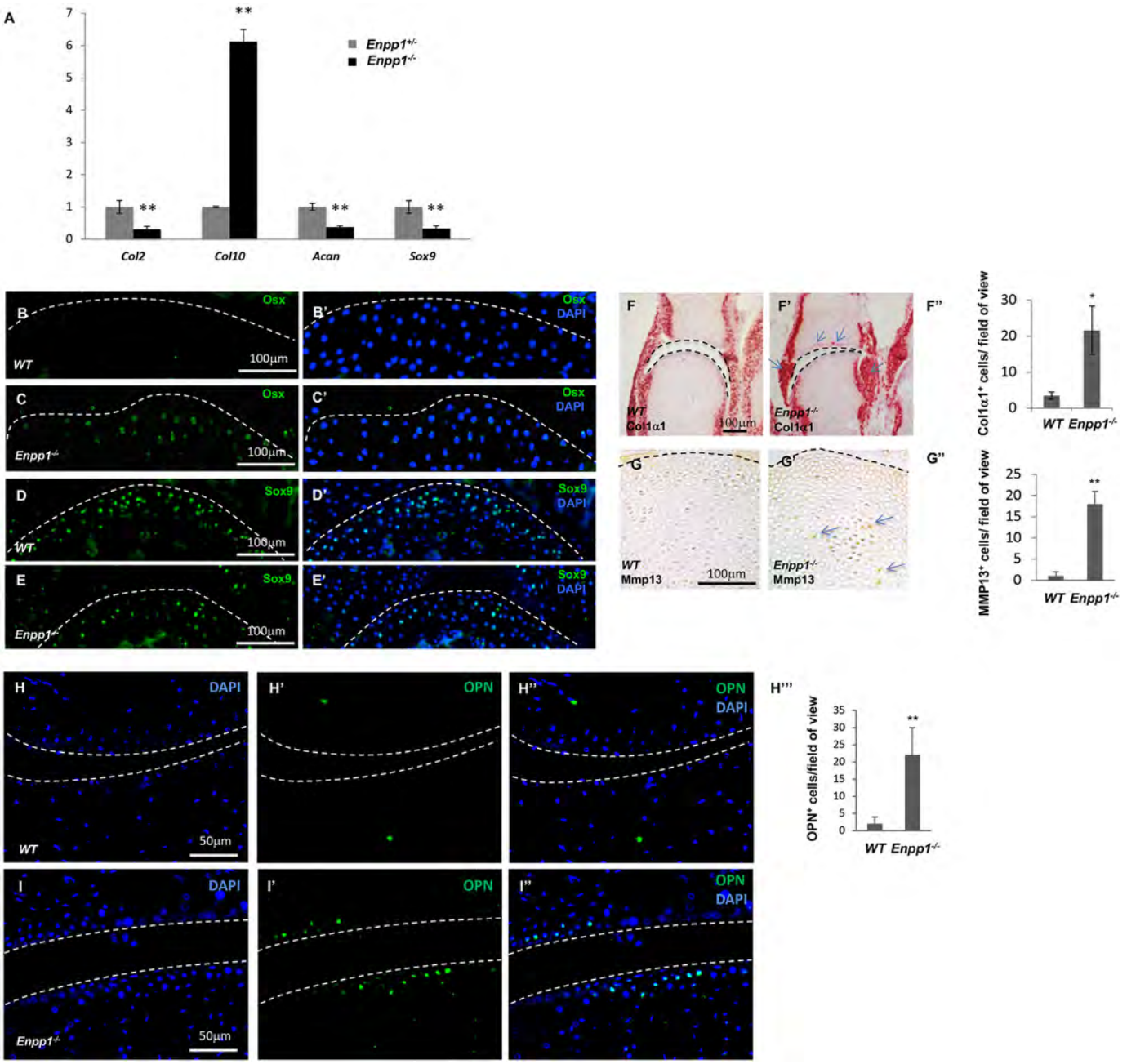

Fig. 1. Ectopic expression of hypertrophic chondrocyte and osteoblast markers in the *Enpp1*$^{-/-}$ metacarpophalangeal joint. (A) qRT-PCR analysis of cartilage-specific markers and hypertrophic markers expressed in the metacarpophalangeal joints of *Enpp1*$^{-/-}$ and WT control mice (*Enpp1*$^{+/-}$) at 1 month of age (n=3). (B-E′) Phalangeal joint sections from 1-month-old WT and *Enpp1*$^{-/-}$ mice were stained with antibodies against Osx (B-C′) and Sox9 (D-E′). Nuclei are stained with DAPI. (F-F″) *Col1a1* mRNA expression detected by ISH with RNAscope technology in the metacarpophalangeal joint surface of newborn pups (P2). Arrows indicate ectopic expression of *Col1a1* in the *Enpp1*$^{-/-}$ joint cartilage and capsule. *Col1a1*-expressing cells in the articular cartilage of the metacarpophalangeal joints were quantified as the number of Col1a1^{+}/field of view under 40× objective magnification (n=4). (G-G″) Mmp13 expression in the joints of P2 WT and *Enpp1*$^{-/-}$ mice. Arrows indicate ectopic expression of Mmp13. Mmp13^{+} cells were quantified as the number of Mmp13^{+} cells/field of view (G″). (H-I″) Opn expression in the joints of 1 month old WT and *Enpp1*$^{-/-}$ mice. Opn^{+} cells were quantified as the number of Opn^{+} cells/field of view (500×400 μm) (H‴). **P*<0.05, ***P*<0.01 (Student's *t*-test). Dashed lines indicate the surface of articular cartilage.

differentiation markers such as *Osx*, *Col1a1* and osteocalcin (*Oc*, also known as *Bglap*) (Fig. 3A). We then further examined Hh signaling activity *in situ* in the joint. A *lacZ* 'knock-in' null allele of *Ptch1* (Mak et al., 2008b) was used to examine *Ptch1* expression. X-gal staining of the *Ptch1*$^{+/-}$ metacarpophalangeal joints at P2 showed *Ptch1-lacZ* expression in the growth plate and perichondrium region as expected (Fig. 3B,C, Fig. S2E). *Ptch1-lacZ* expression in the articular cartilage was much weaker. Interestingly, clustered strong ectopic *Ptch1-lacZ* expression was detected in the articular cartilage and perichondrum (Fig. 3B′-C″, Fig. S2F-F′) in the P2 *Ptch1*$^{+/-}$; *Enpp1*$^{-/-}$ mouse pups. These results indicate that Hh signaling is indeed ectopically activated early after birth in the joint cartilage of the *Enpp1*$^{-/-}$ mice.

As joint mineralization was observed later than Hh signaling upregulation in the *Enpp1*$^{-/-}$ mice, we hypothesized that upregulation of Hh signaling activity may be progressively more

Development (2018) 145, dev164830. doi:10.1242/dev.164830

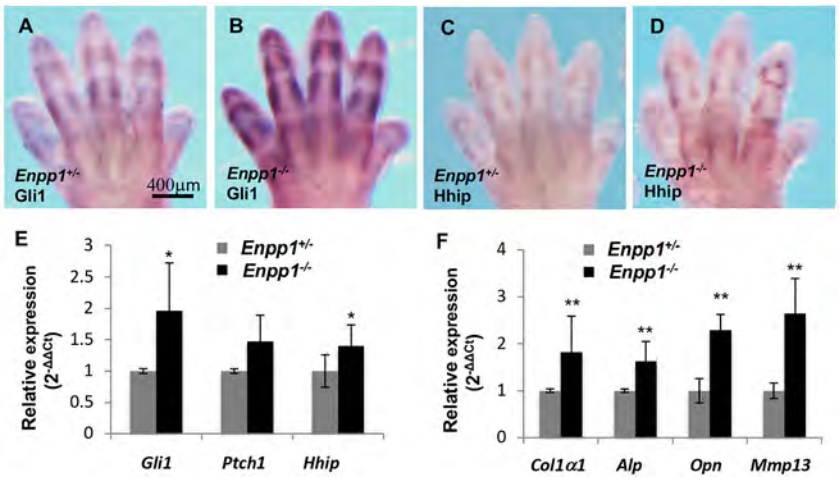

Fig. 2. Increased Hh signaling activity in the *Enpp1*$^{-/-}$ embryo. (A-D) Expression of Hh signaling targets *Gli1* (A,B) and *Hhip* (C,D) in E15.5 WT and *Enpp1*$^{-/-}$ forelimbs shown, by WISH. *Gli1* and *Hhip* mRNA levels were upregulated in the limbs of the *Enpp1*$^{-/-}$ embryos. (E-F) qRT-PCR analysis of Hh target gene expression in the forelimbs of E15.5 embryos (n=3). *P<0.05, **P<0.01 (Student's t-test).

severe, which eventually leads to ectopic joint mineralization. To test this, we performed qRT-PCR analysis with forelimb tissues from 1-month-old WT, *Enpp1*$^{+/-}$ and *Enpp1*$^{-/-}$ mice (Fig. 3D). A more pronounced increase in the expression of Hh signaling target genes and osteoblast markers was observed in the limbs of *Enpp1*$^{-/-}$ mice compared with that seen in the limbs of the WT control. The WT control and *Enpp1*$^{+/-}$ mice, which never developed a stiff joint phenotype, had similar expression levels of the Hh target genes. To examine ectopic activation of Hh signaling *in situ* in older mice, we examined *Ptch1-lacZ* expression again in the metacarpophalangeal joint of 3-week-old mice, before the detection of ectopic mineralization. We found that *Ptch1-lacZ* expression was increased in the perichondrium and periosteum of the *Enpp1*$^{-/-}$ mutant digit close to the growth plate (compare Fig. 3F with E). In the articular cartilage, more cells, particularly those lining the joint surface, showed stronger *lacZ* expression (β-galactosidase staining) in the *Enpp1*$^{-/-}$*; Ptch1*$^{+/-}$ mice (Fig. 3F′) compared with the *Ptch1*$^{+/-}$ control (Fig. 3E′). It has been reported that the articular cartilage and tendon of the joints were mineralized in the *Enpp1*$^{-/-}$ mutants mice at 3 months of age (Hajjawi et al., 2014; Harmey et al., 2004; Okawa et al., 1998; Zhang et al., 2016). To examine Hh signaling activities at this stage, qRT-PCR analysis was performed using the *Enpp1*$^{-/-}$ forelimb tissue. The results confirmed our finding that Hh target genes were highly expressed in the *Enpp1*$^{-/-}$ joints compared with the controls (Fig. S1C). Our results indicate that, in the *Enpp1*$^{-/-}$ joints, Hh activity is increased and detected ectopically before ectopic mineralization occurs in the postnatal phalangeal joint.

As ectopic calcification and *Ptch1-lacZ* expression were found in the digit joint of the *Enpp1*$^{-/-}$ mice, we further examined Gli1 protein expression in the *Enpp1*$^{-/-}$ and WT joint at 2 months and 4 months using immunofluorescent staining. Gli1 expression is also a readout of Hh signaling activity (Ingham and McMahon, 2001) and we found it was indeed ectopically detected in the nucleus of chondrocytes in the articular cartilage of digit joints of both 2-month-old (Fig. 3G-H‴) and 4-month-old (Fig. S2A-D″) *Enpp1*$^{-/-}$ mice. Taken together, these results suggest that, in the phalangeal joints of the *Enpp1*$^{-/-}$ mice, Hh signaling was upregulated, and that this change was associated with ectopic osteoblast differentiation in the phalangeal joints.

Activation of Hh signaling enhances joint calcification in the *Enpp1*$^{-/-}$ mice

Our observation that the loss of *Enpp1* leads to Hh signaling activation in the phalangeal joint suggests that Hh signaling may be a functional target of *Enpp1* in regulating joint integrity. To test this hypothesis genetically, we first set out to determine whether there were genetic interactions between *Ptch1* and *Enpp1* that cause OA. As *Ptch1* encodes an inhibitory receptor of the Hh signaling pathway (Stone et al., 1996), removing one allele of *Ptch1* provides a sensitized genetic background to better reveal the effects of Hh signaling activation. We reasoned that the digit joint calcification phenotype of the *Enpp1*$^{-/-}$ mice should be enhanced by the loss of one copy of *Ptch1*, if activation of Hh signaling is causative for this phenotype. Therefore, the *Ptch1*$^{+/-}$*; Enpp1*$^{-/-}$ mice were generated and *Col1a1* expression was examined by ISH (Fig. 4A-C′, Fig. S3A-C). *Col1a1* expression was further increased in the articular cartilage on both sides of the metacarpophalangeal joint of the P2 *Ptch1*$^{+/-}$*; Enpp1*$^{-/-}$ mice compared with the *Enpp1*$^{-/-}$ mice. Ectopic expression of Osx, Opn and Oc was determined by immunohistochemistry and found to be further increased in the *Ptch1*$^{+/-}$*; Enpp1*$^{-/-}$ joints compared with the *Enpp1*$^{-/-}$ joints (Fig. 4D-F‴, Fig. S3D-D‴). These results indicate that phenotypes of ectopic chondrocyte hypertrophy and/or osteoblast differentiation in the *Enpp1*$^{-/-}$ mutant joint were further enhanced by genetic enhancement of Hh signaling.

Consistent with increased expression of osteoblast markers in the metacarpophalangeal joint of the *Ptch1*$^{+/-}$*; Enpp1*$^{-/-}$ neonatal mice, in the 3-month-old *Ptch1*$^{+/-}$*; Enpp1*$^{-/-}$ mice, joint calcification indicated by Alizarin Red staining was enhanced compared with the *Enpp1*$^{-/-}$ mice (Fig. 4G-J). The joint size was quantified by measuring the relative size of the metacarpophalangeal joints using ImageJ (imagej.nih.gov/ij/) (Fig. S3E). The relative sizes of the metacarpophalangeal joints of digits two and four were further increased in the *Ptch1*$^{+/-}$*; Enpp1*$^{-/-}$ mice compared with those in the *Enpp1*$^{-/-}$ mice (Fig. 4G-J, n=4). There was no significant difference in the relative size of WT and *Enpp1*$^{+/-}$ joints, and both were smaller than the *Enpp1*$^{-/-}$ and *Ptch1*$^{+/-}$*; Enpp1*$^{-/-}$ joints. In addition, we compared mineralization levels of the hindlimbs from 4-month-old mice by X-ray imaging, which also showed that the loss of one copy of *Ptch1* enhanced calcification in the joint area of the *Enpp1*$^{-/-}$ mice (compare Fig. 4N with L). These results indicate that activation of Hh signaling in the *Enpp1*$^{-/-}$ mice further promoted osteoblast differentiation in the joint. We then examined cartilage matrix integrity by Safranin-O staining of the articular cartilage sections (Kim et al., 2014) (Fig. 4O-Q′). More-severe loss of Safranin-O staining was observed in the metacarpophalangeal joint sections from the *Ptch1*$^{+/-}$*; Enpp1*$^{-/-}$ mice than from the *Enpp1*$^{-/-}$ mice at 3 months (Fig. 4P-Q′). These results indicate that increased Hh

Development (2018) 145, dev164830. doi:10.1242/dev.164830

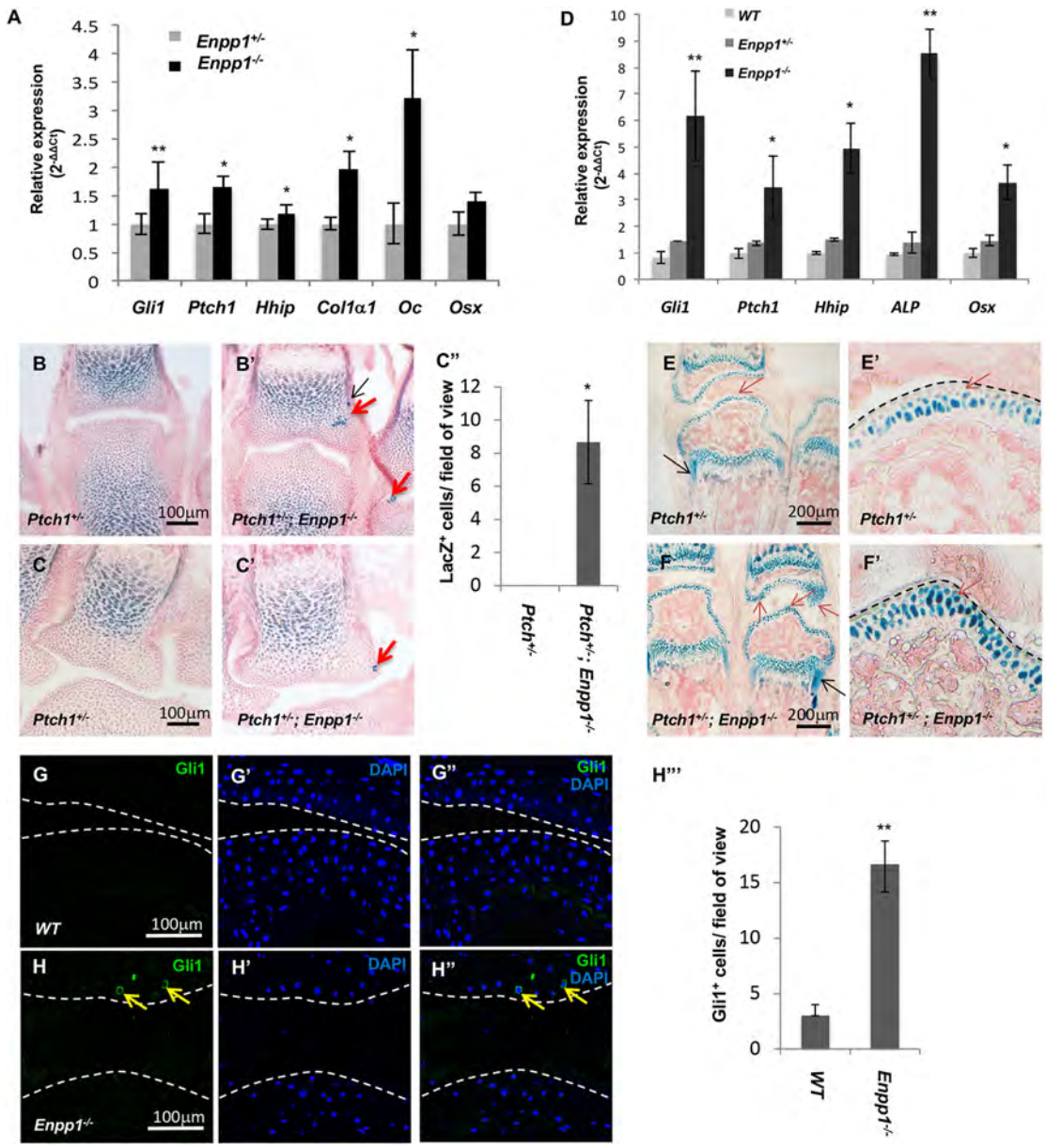

Fig. 3. Increased Hh signaling activity in postnatal *Enpp1*$^{-/-}$ mutant mice. (A) qRT-PCR analysis of gene expression of Hh targets and osteoblast markers in the front paws of P2 mice (n=3). (B-C″) β-galactosidase staining (blue) of the metacarpophalangeal (B,B′) and carpo-metacarpal joints (C,C′) of P2 *Enpp1*$^{-/-}$ and *Enpp1*$^{-/-}$*; Ptch1*$^{+/-}$ mice. Ectopic *Ptch1-lacZ* expression is indicated by red arrows (articular cartilage) and black arrows (perichondrium). The number of *lacZ*$^{+}$ cells in the articular cartilage of the metacarpophalangeal joints was quantified as the number of *lacZ*$^{+}$cells/field of view under 40× objective magnification (n=3) (C″). (D) qRT-PCR analysis of Hh target and osteogenic genes expressed in the front paws of 1-month-old *Enpp1*$^{-/-}$ mice (n=3). (E-F′) Hh signaling activity was detected by *lacZ* expression (β-galactosidase staining, blue) in the metacarpophalangeal joints from 3-week-old *Ptch1*$^{+/-}$ and *Ptch1*$^{+/-}$*; Enpp1*$^{-/-}$ mice. Black arrows indicate Hh activity in the perichondrium of metacarpal bone. The articular cartilage is shown in higher magnification in E′ and F′. Red arrows indicate the *lacZ*$^{+}$ chondrocytes. (G-H‴) Phalangeal joint sections from 2-month-old WT (G-G″) and *Enpp1*$^{-/-}$ (H-H″) mice were stained with antibodies against Gli1. Nuclei are stained with DAPI. Gli1 expression was detected in the articular chondrocyte of *Enpp1*$^{-/-}$ (yellow arrows), but not in WT mice. The number of Gli1^{+} cells in the articular cartilage was quantified as the number of Gli1^{+} cells/field of view under 40× objective magnification (n=3) (H‴). **P*<0.05, ***P*<0.01 (Student's *t*-test). Dashed lines indicate the surface of articular cartilage.

signaling further enhanced the articular cartilage damage and joint calcification that is caused by *Enpp1* loss.

Reduced Hh signaling activity partially rescues joint calcification in the *Enpp1*$^{-/-}$ mice

As Hh signaling promotes chondrocyte hypertrophy as well as osteoblast differentiation (Lin et al., 2009; Mak et al., 2008b; Regard et al., 2013), we next asked whether joint calcification in the *Enpp1*$^{-/-}$ mice can be reduced by inhibiting Hh signaling activity. Gli2 is mainly responsible for the activated form of the Gli transcription factors that activate Hh signaling target gene expression (Ahn and Joyner, 2004; Bai et al., 2002, 2004; Corrales et al., 2004; Joeng and Long, 2009). To reduce Hh activity in the *Enpp1*$^{-/-}$ mice, we removed one copy of *Gli2* (Fig. 5D,D′,H), and found that this led to a decrease in joint sizes compared with those in the *Enpp1*$^{-/-}$ mice (n=4 in each group) (Fig. 5A-D′,I, Fig. S4A-C). *Enpp1*$^{+/-}$*; Gli2*$^{+/-}$ mice or *Enpp1*$^{+/-}$ mice did not show joint calcification and they were considered

Development (2018) 145, dev164830. doi:10.1242/dev.164830

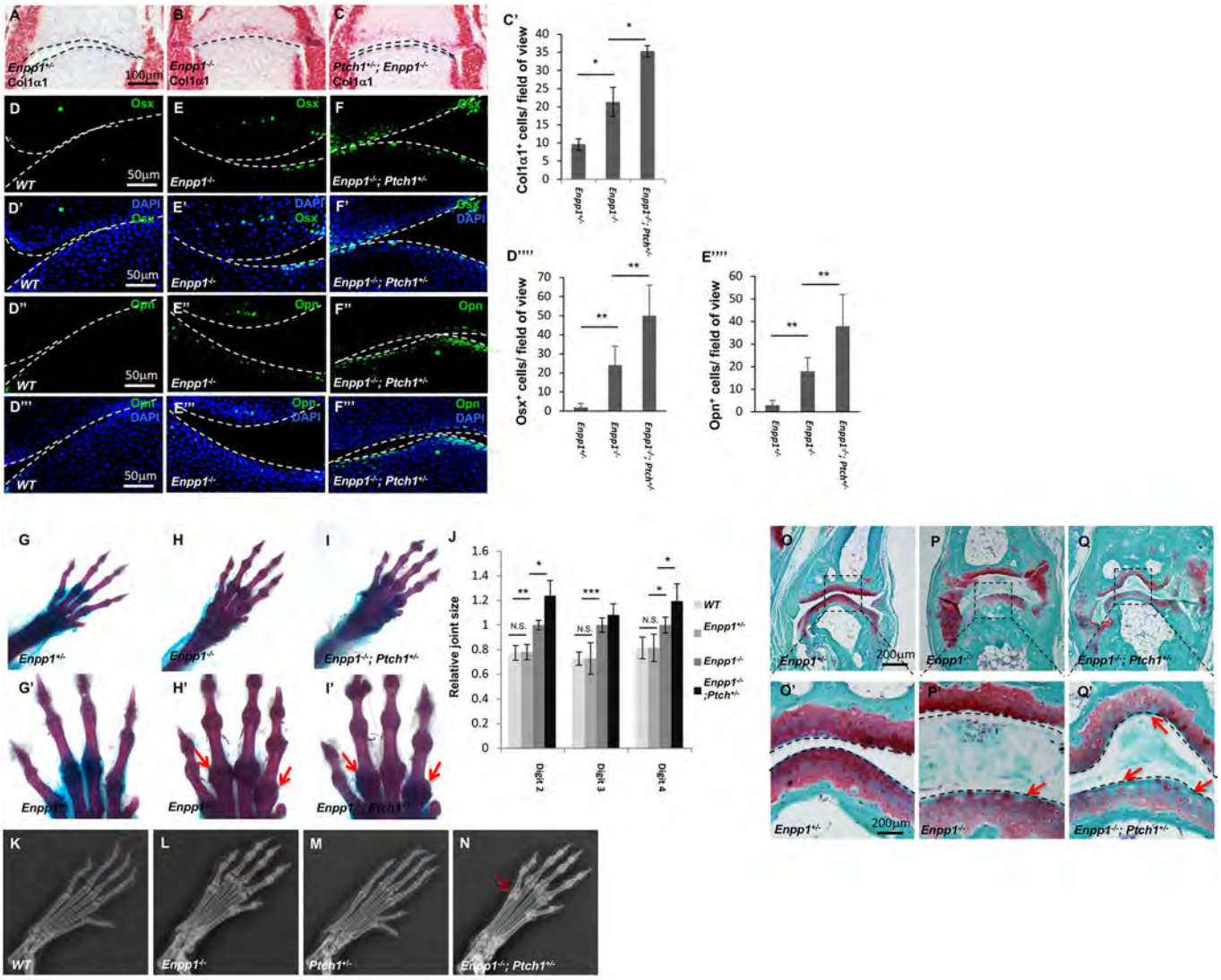

Fig. 4. Enhanced joint calcification by increasing Hh signaling in the *Enpp1*$^{-/-}$ mice. (A-C) *Col1a1* expression was detected using ISH of the phalangeal joint sections from P2 mice. (C′) The number of Col1a1^{+} cells in the articular cartilage of the metacarpophalangeal joints was quantified as the number of Col1a1^{+} cells/field of view under 40× objective magnification (n=3). (D-F‴) Fluorescent immunostaining of Osx and Opn in the phalangeal joint sections of WT, *Enpp1*$^{-/-}$ and *Enpp1*$^{-/-}$*; Ptch1*$^{+/-}$ mice, which were P2 littermates. Osx^{+} and Opn^{+} cells were quantified as the number of Osx^{+} cells/field of view (500×300 µm) (D⁗) and Opn^{+} cells/field of view (500×300 µm) (E⁗). (G-I′) Representative images of Alcian Blue- and Alizarin Red-stained forelimbs from 3-month-old *Enpp1*$^{+/-}$ (G), *Enpp1*$^{-/-}$ (H), and *Enpp1*$^{-/-}$*; Ptch1*$^{+/-}$ (I) mice. Phalangeal joints are shown at higher magnification (G′,H′,I′). Arrows indicate the enlarged metacarpophalangeal joints. (J) Quantification of the size of metacarpophalangeal joints in WT, *Enpp1*$^{+/-}$, *Enpp1*$^{-/-}$*; Ptch1*$^{+/-}$ and *Enpp1*$^{-/-}$ mice. Littermates of *Enpp1*$^{-/-}$*; Ptch1*$^{+/-}$ and *Enpp1*$^{-/-}$ were used in this experiment (n=3). (K-N) Representative X-ray images of the hindlimbs of 4-month-old mice. Arrow indicates enhanced calcification in the phalangeal joint of *Enpp1*$^{-/-}$*; Ptch1*$^{+/-}$ mice. (O-Q′) Safranin-O staining of sections of the metacarpophalangeal joints from forelimbs of 3-month-old *Enpp1*$^{+/-}$ (O,O′), *Enpp1*$^{-/-}$ (P,P′), *Enpp1*$^{-/-}$*; Ptch1*$^{+/-}$ (Q,Q′) mice. Arrows indicate reduced Safranin-O staining. O′,P′,Q′ are enlargements of the boxed areas in O,P,Q, respectively. NS, not significant, *P<0.05, **P<0.01 (Student's t-test). Dashed lines indicate the surface of articular cartilage.

control groups (Fig. 5A-B′). As Hh signaling promotes osteoblast differentiation from mesenchymal progenitor cells, we next tested whether *Enpp1* inhibits osteoblast differentiation from mesenchymal progenitor cells by inhibiting Hh signaling. Subcutaneous mesenchymal progenitors (SMPs) were isolated from the *Enpp1*$^{-/-}$*; Gli2*$^{+/-}$, *Enpp1*$^{-/-}$, *Enpp1*$^{+/-}$*; Gli2*$^{+/-}$ and *Enpp1*$^{+/-}$ mice, and cultured under osteogenic conditions. Osteoblast differentiation was determined by alkaline phosphatase (ALP) staining and qRT-PCR assays. ALP activity was similar in the control *Enpp1*$^{+/-}$*; Gli2*$^{+/-}$ and in the *Enpp1*$^{+/-}$ SMPs, but increased in the *Enpp1*$^{-/-}$ SMPs. This increase was ameliorated in the *Enpp1*$^{-/-}$*; Gli2*$^{+/-}$ cells (Fig. 5E-H). Consistently, expression of Hh target genes and osteogenic markers were all decreased in the *Enpp1*$^{-/-}$*; Gli2*$^{+/-}$ SMPs compared with the *Enpp1*$^{-/-}$ SMPs (Fig. 5J). Therefore, reduction of Hh signaling indeed led to a reduction in osteoblast differentiation from mesenchymal progenitor cells promoted by loss of *Enpp1*.

Loss of *Gnas*-enhances joint calcification in the *Enpp1*$^{-/-}$ mice

As Hh signaling activation due to *Enpp1* loss contributed to joint calcification in the *Enpp1*$^{-/-}$ mice, we next asked how Enpp1 inhibits Hh signaling. The Hh signaling pathway can be inhibited by

Development (2018) 145, dev164830. doi:10.1242/dev.164830

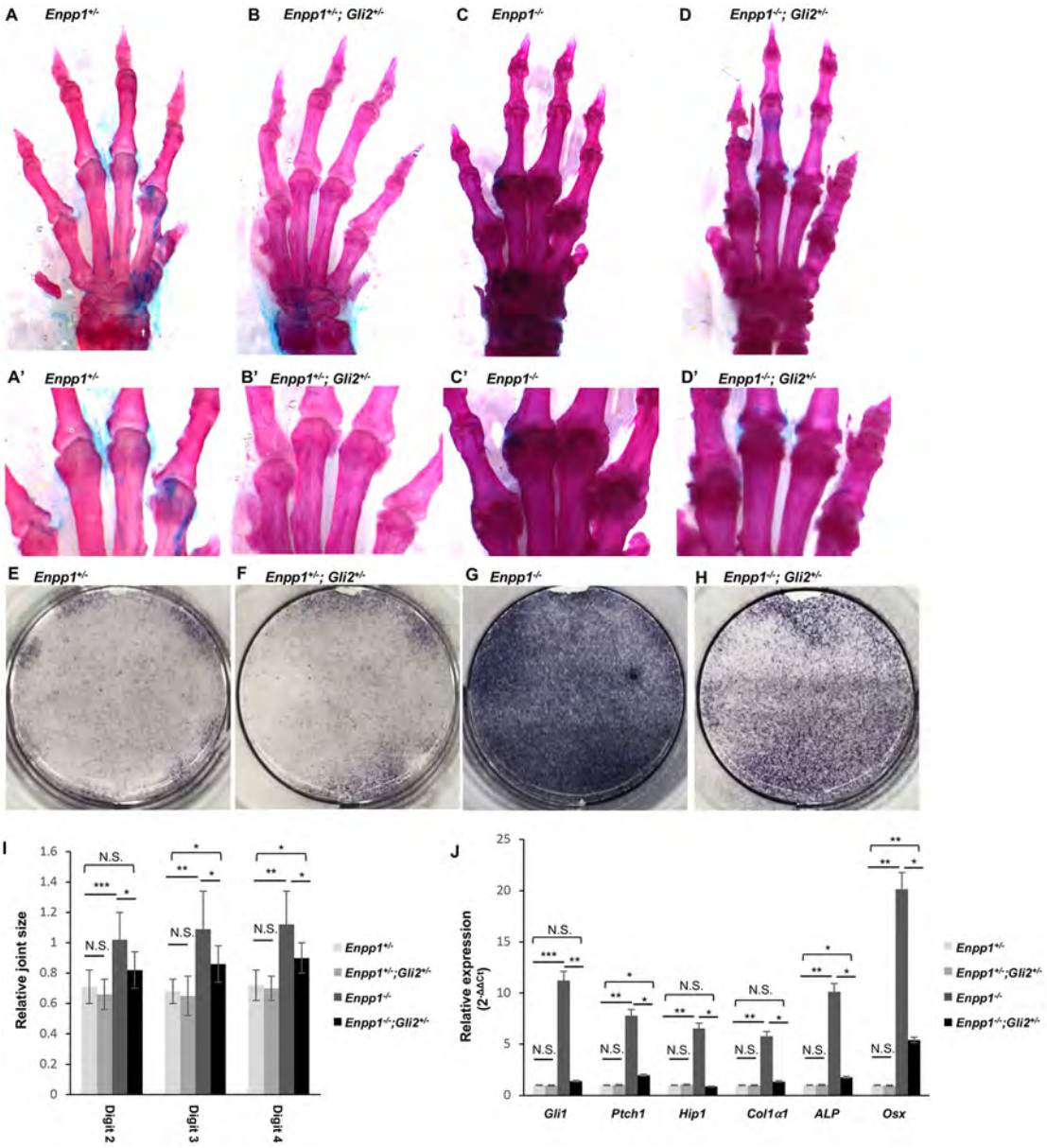

Fig. 5. Reduced Hh signaling activity partially rescued joint calcification of *Enpp1*$^{-/-}$ mice. (A-D) Representative images of Alcian Blue and Alizarin Red stained forelimbs from 3-month-old *Enpp1*$^{-/-}$ (A), *Enpp1*$^{+/-}$; *Gli2*$^{+/-}$ (B), *Enpp1*$^{-/-}$ (C) and *Enpp1*$^{-/-}$; *Gli2*$^{+/-}$ (D) mice. (A′,B′,C′,D′) Phalangeal joints shown at higher magnification. (E-G) Representative ALP staining of SMPs from WT (E), *Enpp1*$^{+/-}$; *Gli2*$^{+/-}$ (F), *Enpp1*$^{-/-}$ (G) and *Enpp1*$^{-/-}$; *Gli2*$^{+/-}$ mice (H) cultured in osteogenic medium for 7 days. (I) Quantification of the relative metacarpophalangeal joint sizes. Littermates were used in this experiment, *n*=4. (J) qRT-PCR analysis of Hh target and osteoblast genes expressed in SMPs of indicated genotypes. SMPs were cultured in osteogenic medium for 7 days (*n*=3). NS, not significant, **P*<0.05, ***P*<0.01, ****P*<0.001 (Student's *t*-test).

$G\alpha_s$ signaling (He et al., 2014; Regard et al., 2013) and ATP can signal through $G\alpha_i$- or $G\alpha_s$-coupled receptors (Burnstock, 2007; Di Virgilio, 2012). We therefore tested whether ectopic joint calcification in the *Enpp1*$^{-/-}$ mice can be enhanced by loss of *Gnas* function. The *Enpp1*$^{-/-}$; *Gnas*$^{+/-}$ mice were generated, and ectopic calcification of the metacarpal bones and interphalangeal joints were examined at 2 months of age (Fig. 6A-D) (*n*=3 in each group). Ectopic calcification was not detected in the *Gnas*$^{+/-}$ mice (Fig. 6C), but the loss of one copy of *Gnas* enhanced joint calcification of the *Enpp1*$^{-/-}$ mice (compare Fig. 6D with B). This was also confirmed by Alizarin Red and Alcian Blue staining of the skeleton of 2.5-month-old mice (Fig. 6E,F). The *Enpp1*$^{-/-}$; *Gnas*$^{+/-}$ mice showed the most-severe calcification and enlargement of the interphalangeal joints, with reduced space in the phalangeal joint cavity.

We then performed Safranin-O staining of the phalangeal joint sections to detect the cartilage matrix integrity. Articular cartilage was thinner at 1 month in the *Enpp1*$^{-/-}$; *Gnas*$^{+/-}$ joints compared with the joint from the *Enpp1*$^{-/-}$ mice (Fig. 6G-I). A thinner articular cartilage layer in the joint was also found in the *Ptch1*$^{c/c}$; *Col2a1-CreER* mice (Mak et al., 2008b), consistent with the notion that upregulated Hh signaling contributes to the joint phenotypes. To test whether a reduction of *Gnas* is associated with Hh signaling upregulation, we examined expression of Gli1, Osx and Sox9 by immunohistochemistry. We found that, whereas Gli1 and Osx were expressed at higher levels in the articular cartilage of the *Enpp1*$^{-/-}$;

Development (2018) 145, dev164830. doi:10.1242/dev.164830

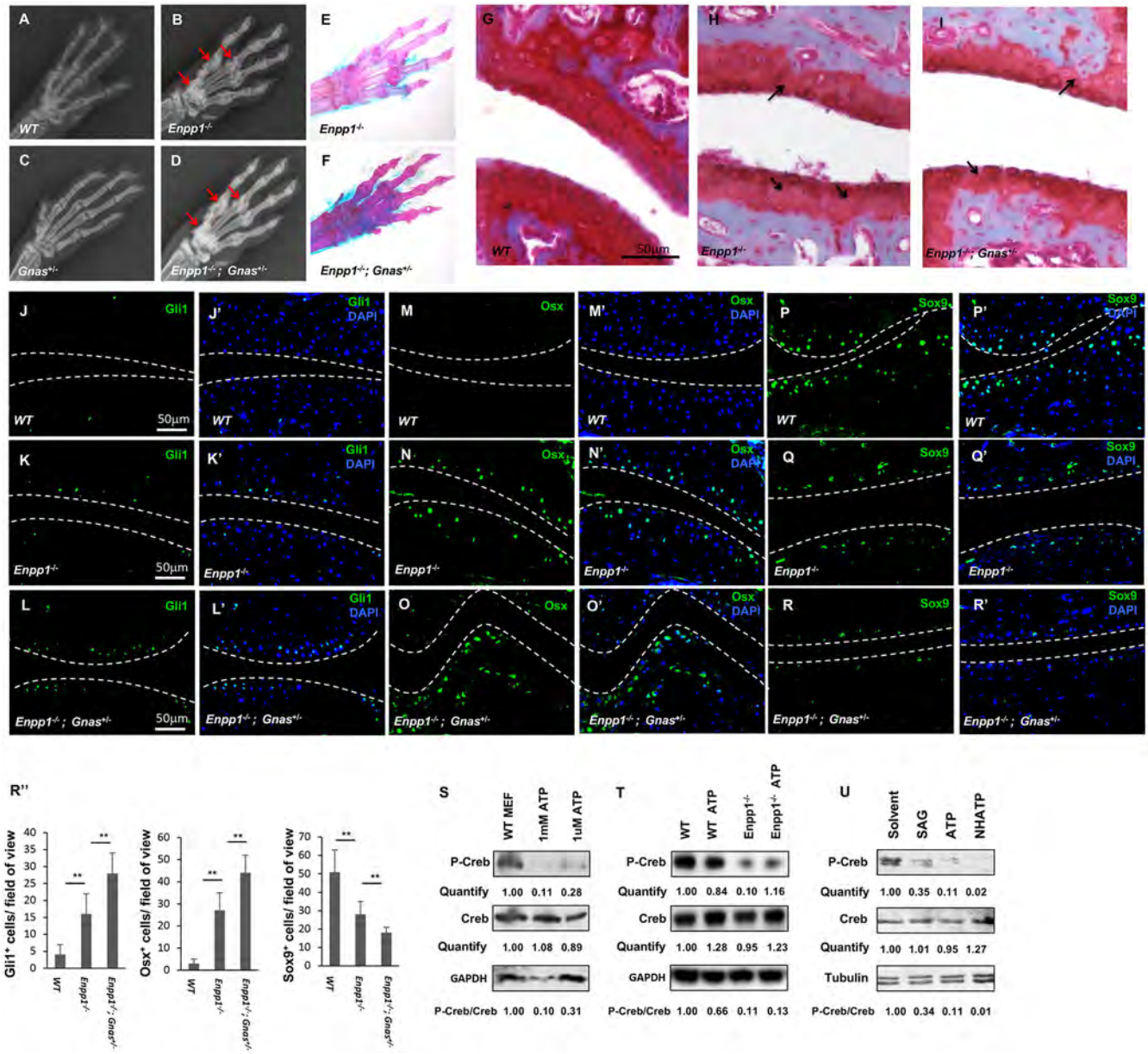

Fig. 6. Ectopic joint calcification in *Enpp1*$^{-/-}$ mutants was enhanced by reduced *Gnas*. (A-D) Representative X-ray images of the forelimbs of 2-month-old WT, *Enpp1*$^{-/-}$, *Gnas*$^{+/-}$ and *Enpp1*$^{-/-}$*; Gnas*$^{+/-}$ mice. *Gnas*$^{+/-}$ enhanced the joint calcification of the *Enpp1*$^{-/-}$ mice. These data indicated that Enpp1 may signal through Gα_s in regulating cartilage calcification. Arrows indicate calcified joints. (E-F) Representative Alizarin Red and Alcian Blue staining of forelimbs from the *Enpp1*$^{-/-}$ and the *Enpp1*$^{-/-}$*; Gnas*$^{+/-}$ mice at 2.5 months of age. More ectopic mineralization can be found around the joints of the *Enpp1*$^{-/-}$*; Gnas*$^{+/-}$ mice compared with the *Enpp1*$^{-/-}$ mice. (G-I) Representative Safranin-O staining of phalangeal joint sections from forelimbs of 1-month-old mice. Arrows indicate reduced Safranin-O staining and reduced cartilage thickness. (J-R″) Sections of phalangeal joints from 1-month-old WT, *Enpp1*$^{-/-}$ and *Enpp1*$^{-/-}$*; Gnas*$^{+/-}$ mice were stained with antibodies against Gli1 (J-L′), Osx (M-O′) and Sox9 (P-R′). Gli1, Osx and Sox9 positive cells were counted and quantified as the number of Gli1$^+$/field of view, Osx$^+$/field of view and Sox9$^+$/field of view (500×400 μm) (R″). Nuclei are stained with DAPI. (S) Western blot PKA activity measured using p-Creb levels in MEF cells from WT mice. Cells were treated for 5 min with ATP of indicated concentration. (T) Chondrocytes isolated from P0 WT and *Enpp1*$^{-/-}$ mice were treated with 1 mM ATP for 5 min. P-Creb and total Creb protein levels were detected using western blotting. (U) WT MEF cells were treated with 100 nM SAG, 0.1 mM ATP or 0.1 mM NHATP for 10 min. p-Creb, total Creb and tubulin protein levels were detected using western blotting. Protein bands in the blot were quantified by densitometry and analyzed using ImageJ. The numbers indicate relative grayscale values of P-Creb and Creb in each lane, and P-Creb/Creb ratio was calculated. ***P*<0.01 (Student's *t*-test). Dashed lines indicate the surface of articular cartilage.

Gnas$^{+/-}$ mice than in the *Enpp1*$^{-/-}$ mice, Sox9 expression was reduced (Fig. 6J-R″). These results indicate that *Gnas* genetically interacts with *Enpp1* to inhibit joint calcification, and support the suggestion that Enpp1 may act through Gα_i to inhibit Hh signaling in the joint cartilage.

The P2 purinergic receptors (i.e. P2X and P2Y receptors) mediate ATP signaling (Erb et al., 2006; Khakh and North, 2006). Eight P2Y family members are GPCRs (P2Y1, P2Y2, P2Y4, P2Y6, P2Y11, P2Y12, P2Y13 and P2Y14) and they respond to the extracellular ATP and ADP (North, 2002). In addition, adenosine receptors, which are also GPCRs, respond to adenosine derived from ATP and ADP after hydrolysis. To test whether ectopic calcification in the *Enpp1*$^{-/-}$ mice may be caused by increased extracellular ATP, which can act through Gα_i-coupled P2 purinergic

Development (2018) 145, dev164830. doi:10.1242/dev.164830

receptors to inhibit cAMP production and protein kinase A (PKA) activity, we treated mouse embryonic fibroblast (MEF) cells with ATP and measured p-Creb levels as an indication of PKA activities, which are positively or negatively regulated by $G\alpha_s$ or $G\alpha_i$ through cAMP, respectively. MEF cells were treated with 1 mM or 1 µM of ATP for 5 min. The p-Creb levels were significantly decreased by both ATP treatments, especially after the 1 mM ATP treatment (Fig. 6S). To test whether joint cells were similarly regulated, ATP treatment of primary synovial cells was performed, which also resulted in reduction of Creb phosphorylation (Fig. S4D). These results suggest that increased extracellular ATP can decrease cAMP and PKA levels, leading to a reduction of p-Creb levels. To further test whether chondrocytes were regulated by Enpp1 through ATP, primary chondrocytes were isolated from the WT or *Enpp1*$^{-/-}$ mice and treated with vehicle (doubly distilled H_2O) or 1 mM ATP for 5 min. ATP treatment of WT chondrocytes also reduced Creb phosphorylation, and *Enpp1*$^{-/-}$ chondrocytes with vehicle treatment showed a much lower p-Creb/total Creb ratio compared with those from the WT chondrocytes (Fig. 6T), indicating that the loss of Enpp1 in chondrocytes leads to a reduction of PKA activity due to increased extracellular ATP levels. Furthermore, *Enpp1*$^{-/-}$ chondrocytes did not respond to ATP treatment (Fig. 6T), possibly because of saturated ATP levels. These results suggest that, in chondrocytes and possibly other synovial tissues, Enpp1 regulates PKA activity, which in turn regulates Hh signaling, as has been previously reported in other contexts (He et al., 2014; Regard et al., 2011, 2013).

ATP can be hydrolyzed by Enpp1 to form PP_i and AMP, which can be further hydrolyzed to form adenosine and P_i. To further test whether loss of Enpp1 leads to increased ATP signaling through $G\alpha_i$ to decrease p-Creb, we treated MEF cells with ATP and a non-hydrolyzeable ATP (NHATP; β, γ-CH_2-ATP), which functions as a selective inhibitor of human ENPP1 (Lecka et al., 2013). In the MEF cells, we found that both ATP and NHATP can efficiently reduce the phosphorylation of Creb at the concentration of 0.1 mM for 10 min (Fig. 6U). NHATP appears to have a slightly stronger action than ATP, possibly due to its resistance to hydrolysis. Interestingly, treatment with SAG, an agonist of Hh receptor smoothened (a seven transmembrane protein), also reduced Creb phosphorylation. These results suggest that Enpp1 in the extracellular space may promote $G\alpha_s$ signaling activity by reducing ATP-induced $G\alpha_i$ signaling, thereby inhibiting joint calcification.

DISCUSSION

Here, we show that upregulated Hh signaling activity contributes to the joint calcification phenotypes of *Enpp1*$^{-/-}$ mice. Increased Hh signaling activity was observed early in development of the *Enpp1*$^{-/-}$ embryos. Ectopic expression of Hh target genes, together with upregulation of chondrocyte hypertrophy and/or osteogenic markers, preceded calcification in the joint of the postnatal *Enpp1*$^{-/-}$ mice. Genetic enhancement or reduction of Hh signaling enhanced or reduced the joint calcification phenotypes in the *Enpp1*$^{-/-}$ mice, respectively. Our work suggests that inhibition of Hh signaling may lead to a therapeutic strategy to reduce ectopic calcification caused by loss or reduced ENPP1 functions in humans.

Extracellular PP_i is a crucial factor that inhibits calcification. Enpp1 deficiency directly leads to reduced PP_i levels, causing the deposition of hydroxyapatite (Murshed et al., 2005; Harmey et al., 2004). In this current study, we observed activation of Hh signaling and expression of chondrocyte hypertrophy and/or osteoblast markers in the *Enpp1*$^{-/-}$ joint, indicating that calcification caused by *Enpp1* deficiency is not only a process of passive deposition of hydroxyapatite on the joint surface, but is also driven by an active process due to ectopic chondrocyte hypertrophy and/or osteoblast differentiation driven by activated Hh signaling. As recent studies show that chondrocytes can transdifferentiate into osteoblasts (Dy et al., 2012; Park et al., 2015; Yang et al., 2014a,b; Zhou et al., 2014), it will be interesting to further determine whether osteoblast transdifferentiation indeed occurs in the articular cartilage of *Enpp1*$^{-/-}$ mice. Our evidence suggests that Hh signaling upregulation is a primary outcome of *Enpp1* deficiency, not a secondary effect of decreased PP_i, as both ATP and NHATP inhibited PKA activity, shown by reduced Creb phosphorylation (Fig. 6U). It is likely that decreased PPi levels and Hh signaling activation are two parallel processes that induced calcification. This is further supported by partial rescue of ectopic calcification in the *Enpp1*$^{-/-}$ mice by removing one copy of *Gli2*. There are several possibilities for why *Gli2*$^{+/-}$ only partially rescued the *Enpp1*$^{-/-}$ stiff joint phenotype. First, whole-body PP_i levels were decreased in the *Enpp1*-deficient mice (Johnson et al., 2003). Removal of *Gli2* cannot change the circulating P_i/PP_i ratio in the *Enpp1*$^{-/-}$; *Gli2*$^{+/-}$ mice, as Hh signaling and PP_i act in parallel downstream of *Enpp1*. Second, although we removed *Gli2*, *Gli1* and *Gli3* are still there to transduce Hh signaling. Lastly, *Enpp1* may regulate other signaling pathways to inhibit osteoblast differentiation.

Hh signaling plays crucial roles in regulating chondrocyte proliferation and hypertrophy during embryonic development and after birth. Ectopic activation of Hh signaling causes OA in long bone synovial joints (Lin et al., 2009; Mak et al., 2008a). Our findings extend these previous studies by showing that Enpp1 is an important regulator of Hh signaling. Joint calcification was detected in the phalangeal joint cartilage and the soft tissue, such as the joint capsule in the *Enpp1*$^{-/-}$ mice. Similar observations have been made in a recent study showing that *Enpp1* loss of function leads to ectopic mineralization in cartilage and soft tissues, such as tendons and ligaments (Hajjawi et al., 2014; Harmey et al., 2004; Zhang et al., 2016). Our results suggest that upregulated Hh signaling activity in the absence of *Enpp1* may be a common mechanism underlying ectopic calcification that is found in distinct tissues. In addition to joint calcification, the loss of *Enpp1* function also results in vascular calcification (Lorenz-Depiereux et al., 2010; Rutsch et al., 2003), a degenerative process that is associated with an increased risk of cardiovascular problems. Humans who carry the *ENPP1* loss of function mutations develop the vascular calcification GACI (Nitschke et al., 2012), which is a rare autosomal-recessive disorder with calcification of the internal elastic lamina and fibrotic myointimal proliferation of muscular arteries (Rutsch et al., 2001). It would be interesting to determine whether arterial calcification and joint calcification share similar mechanisms involving the activation of Hh signaling, and whether inhibition of Hh signaling could reduce vascular calcification.

MATERIALS AND METHODS

Animals and diet

The mouse lines have been described previously: *Enpp1*$^{-/-}$ mice (*C57BL/6-Enpp1tm1*) (Serrano et al., 2014); *Gnas*$^{f/f}$ (Chen et al., 2005), *Ptch1*$^{+/-}$ (Mak et al., 2008a), *Gli2*$^{+/-}$ (Bai and Joyner, 2001) and *Osx-GFP::Cre* mice (Rodda and McMahon, 2006). Genotyping was carried out using tail genomic DNA by standard PCR-based procedures. Mice were maintained on normal laboratory diet. Mice of the same genetic background were generated and raised under identical conditions. Female and male mice exhibited similar phenotypes. As the genetic experiments require a large number of females to breed the appropriate number of mice with desired genotypes, we only used males for experiments. Sex-matched littermate mice were compared. All mouse experiments were approved by the Institutional Animal Care

Development (2018) 145, dev164830. doi:10.1242/dev.164830

and Use Committee of the National Institutes of Health and Harvard Medical School.

Histological analysis of the interphalangeal joints

Histological analysis was performed on the paraffin sections of the metacarpophalangeal joints of the forelimbs. Skeletal tissues were fixed in 4% paraformaldehyde (PFA) (wt/vol) overnight at 4°C, decalcified for 1 week in 0.5 M EDTA (pH 8.0) and dehydrated. Paraffin-embedded tissue was sectioned at 7 µm and stained with Safranin-O and Hematoxylin & Eosin according to standard procedures. Whole-mount X-gal staining was performed as has been previously described (Topol et al., 2003).

Radiography of skeleton

X-ray images of the fixed forelimbs were taken using the Bruker MS FX PRO Imager.

Immunostaining

Forelimbs were collected and immediately fixed in 4% PFA (wt/vol) overnight at 4°C. Then limbs were decalcified in 0.5 M EDTA (pH 7.4) for 2 weeks at 4°C, changing EDTA every 3-4 days. The limbs were placed in 30% (wt/vol) sucrose at 4°C overnight, embedded in optimal cutting temperature compound and sectioned at 16 µm. The slides were blocked in 5% bovine serum albumin (BSA) (wt/vol) in PBST (PBS with 0.02% Tween-20) at room temperature for 1 h, then incubated with primary antibodies diluted in blocking buffer overnight at 4°C. The slides were washed in PBST for 3×10 min, incubated in secondary antibodies for 1 h at room temperature and washed in PBST for 3×10 min before imaging. Primary antibodies that were used in immunostaining include: anti-Gli1 (Santa Cruz Biotechnology, sc-6152) at 1:50, anti-Col1a1 (Santa Cruz Biotechnology, sc-59772) at 1:500, anti-Osx (Abcam, 22552) at 1:400, anti-Opn (R&D Systems, AF808) at 1:500, anti-Oc (LifeSpan BioSciences, LS-C42094) at 1:100 and anti-Sox9 (Abcam, 185966) at 1:400. To quantify immunostaining, the immunopositive cells in a field of view that had a greater intensity than the background were counted using Photoshop CS6. The total area of each field of view was calculated using ImageJ, and at least three fields of view were counted for each immunostaining.

Isolation, culturing and analyses of SMP, MEF, chondrocytes and synoviocytes

Subcutaneous skin tissue containing adipose deposits were dissected from 6-week-old mice. The subcutaneous tissue was prepared under sterile conditions and washed in PBS supplemented with 100 U/ml penicillin and 100 µg/ml streptomycin on ice. Tissue was minced and digested with 1 mg/ml collagenase type 1 and 0.5% trypsin in 0.1% BSA at 37°C for 2 h, then centrifuged at 650 ***g*** for 10 min. The floating fat depots were removed, and the cell pellets were collected, dissociated and centrifuged a second time at 650 ***g*** for 10 min. The SMP cell pellet was dissociated and filtered through a 100 µm mesh filter. SMP cells were cultured in Alpha-MEM with 20% fetal bovine serum, 100 U/ml penicillin, 100µg/ml streptomycin and 2 mM glutamine. Cells were seeded at a density of 2.5×10^5 per well in 12-well plates and switched into osteogenic medium with ascorbic acid and glycerophosphate after reaching super confluence. MEF cells were isolated from E12.5-13.5 mouse embryos. The internal organs of the embryos were removed from the abdominal cavity. Embryos were rinsed in 10-20 ml Dulbecco's phosphate-buffered saline and transferred to a 15 ml tube containing 3-5 ml trypsin/EDTA solution and incubated for 20 min at 37°C. The digested cells were collected and large tissue pieces were avoided. The suspended cells were then centrifuged for 5 min at 1000 ***g*** at room temperature. The cells in the pellets were dissociated in 10-50 ml fresh MEF medium with penicillin/streptomycin and plated in 100 mm tissue culture plates or 75 cm^2 flasks. Primary chondrocytes were isolated from P0 mice. The rib cages were incubated with pronase for 30 min at 37°C, followed by 3 mg/ml collagenase in Dulbecco's modified eagle medium (DMEM) at 37°C for 1 h 30 min until all soft tissues could be detached from the cartilage by a small amount of pipetting. The cartilage was digested with collagenase for 4-5 h and chondrocytes were harvested by centrifugation. Synovial cells were isolated from synovial membranes of the knee joints of 10-week-old mice after digestion with 0.2% collagenase in DMEM at 37°C for 1 h. The treatment was carried out using ATP (Sigma FLAAS-1VL), NHATP (Sigma-Aldrich, A2647) and SAG (MedChem Express, HY-12848). Western blotting analysis was performed according to standard protocols (Jin et al., 2012). Antibodies used were: rabbit anti-p-Creb (1:2000; Millipore, 06-519), rabbit anti-Creb (1:2000; Santa Cruz Biotechnology, sc-25785), mouse anti-GAPDH (1:5000; Sigma-Aldrich, G8795) and mouse anti-tubulin (1:5000; Sigma-Aldrich, T5168).

Quantitative RT-PCR

Quantitative RT-PCR was performed to measure the relative mRNA levels. RNA samples were prepared from the forelimbs without skin using Trizol (Invitrogen) with the RNeasy kit (Qiagen). The phalangeal joints between the metacarpal bone and the proximal phalanx of digit three were used for analysis, unless otherwise indicated in the text. cDNA was generated by the SuperScript2 reverse transcriptase kit (Invitrogen) and digested with DNase1 (Invitrogen). Primers used for amplification have been described previously (Regard et al., 2013). Samples were normalized with GAPDH expression.

Whole-mount skeletal preparation and joint size measurements

Mice were skinned and placed in 100% ethanol overnight, then in 100% acetone for 1 day. Whole-mount skeletal preparations were performed as described (McLeod, 1980). Mice were then stained with Alcian Blue and Alizarin Red solution (50 ml staining solution=2.5 ml 0.3% Alcian Blue, 2.5 ml 0.1% Alizarin Red, 2.5 ml 100% glacial acetic acid and 42.5 ml 70% ethanol) for 2 days at 37°C. The mice were then cleared in 1% KOH for 2 days and transferred to 20% glycerol with 1% KOH until soft tissue was transparent. The cleared mice were stored in 80% glycerol. Four mice of each genotype were used for quantification of the forelimb metacarpophalangeal joints size. Statistics shown in text are mean±s.d. The joint sizes were measured using ImageJ as follows: the length of a straight line indicates the diameter of metacarpophalangeal joint size (D1) on the frontal view of the forelimb and is measured as pixels. The midpoint of the proximal phalange was visually determined and the diameter of the proximal phalanges (D2) was similarly measured. Then the ratio of D1/D2 of each digit was calculated as the relative joint size and used in the statistical analysis.

In situ hybridization

Forelimbs for ISH were fixed in 10% (vol/vol) formalin at room temperature for 24-36 h. Paraffin sections at 8 µm were used to perform RNA ISH using an RNAscope (ACDBio) (Wang et al., 2012) 2.0HD Detection Kit according to the manufacturer's instructions. The probe used in the study is mCol1α1 (Ref: 319371, Lot:15258A, ACDBio). The intensity of ISH signal across the various anatomical locations was compared. WISH was performed according to an established protocol (Andre et al., 2015).

Statistical analysis

Quantification was performed from at least three independent experimental groups and presented as mean±s.d. Statistical analysis between groups was performed by two-tailed Student's *t*-test to determine significance when only two groups were compared. $P<0.05$ was considered statistically significant ($*P<0.05$, $**P<0.01$, $***P<0.001$). The signal of immunohistochemistry was calculated as the number of positive cells/field of view.

Acknowledgements

We thank members of the Yang lab for stimulating discussions.

Competing interests

The authors declare no competing or financial interests.

Author contributions

Conceptualization: Y.Y.; Methodology: Y.Y., Y.J., Q.C., J.G.-J., R.T.; Validation: Y.Y., Y.J., Q.C., J.G.-J., J.H., Y.Z.; Formal analysis: Y.Y., Q.C., Y.J., J.G.-J., J.H.; Investigation: Y.Y., Y.J., Q.C., J.G.-J., J.H., Y.Z., R.T.; Resources: Y.Y.; Data curation: Q.C., Y.J., J.G.-J., J.H., Y.Z.; Writing - original draft: Y.Y., Y.J.; Writing - review & editing: Y.Y., Q.C., Y.J., R.T.; Supervision: Y.Y.; Project administration: Y.Y.; Funding acquisition: Y.Y.

Funding
The work in the Yang lab was supported by R01DE025866 and R01AR070877 from the National Institutes of Health. Y.J. is also supported by the National Natural Science Foundation of China (81702112), Shanghai Sailing Program (17YF1404900) and the National Key Research and Development Program of China (2016YFC0902102). R.T. is supported by the U.S. Department of Veterans Affairs (I01BX001660) and the National Institutes of Health (AG007996). Deposited in PMC for release after 12 months.

Supplementary information
Supplementary information available online at
http://dev.biologists.org/lookup/doi/10.1242/dev.164830.supplemental

References

Ahn, S. and Joyner, A. L. (2004). Dynamic changes in the response of cells to positive hedgehog signaling during mouse limb patterning. *Cell* **118**, 505-516.
Andre, P., Song, H., Kim, W., Kispert, A. and Yang, Y. (2015). Wnt5a and Wnt11 regulate mammalian anterior-posterior axis elongation. *Development* **142**, 1516-1527.
Arai, M., Anderson, D., Kurdi, Y., Annis-Freeman, B., Shields, K., Collins-Racie, L. A., Corcoran, C., DiBlasio-Smith, E., Pittman, D. D., Dorner, A. J. et al. (2004). Effect of adenovirus-mediated overexpression of bovine ADAMTS-4 and human ADAMTS-5 in primary bovine articular chondrocyte pellet culture system. *Osteoarthritis Cartilage* **12**, 599-613.
Babij, P., Roudier, M., Graves, T., Han, C.-Y. E., Chhoa, M., Li, C.-M., Juan, T., Morony, S., Grisanti, M., Li, X. et al. (2009). New variants in the Enpp1 and Ptpn6 genes cause low BMD, crystal-related arthropathy, and vascular calcification. *J Bone Miner. Res.* **24**, 1552-1564.
Bai, C. B. and Joyner, A. L. (2001). Gli1 can rescue the in vivo function of Gli2. *Development* **128**, 5161-5172.
Bai, C. B., Auerbach, W., Lee, J. S., Stephen, D. and Joyner, A. L. (2002). Gli2, but not Gli1, is required for initial Shh signaling and ectopic activation of the Shh pathway. *Development* **129**, 4753-4761.
Bai, C. B., Stephen, D. and Joyner, A. L. (2004). All mouse ventral spinal cord patterning by hedgehog is Gli dependent and involves an activator function of Gli3. *Dev. Cell* **6**, 103-115.
Bastepe, M., Weinstein, L. S., Ogata, N., Kawaguchi, H., Juppner, H., Kronenberg, H. M. and Chung, U.-I. (2004). Stimulatory G protein directly regulates hypertrophic differentiation of growth plate cartilage in vivo. *Proc. Natl. Acad. Sci. USA* **101**, 14794-14799.
Bertrand, J., Nitschke, Y., Fuerst, M., Hermann, S., Schäfers, M., Sherwood, J., Nalesso, G., Ruether, W., Rutsch, F., Dell'Accio, F. et al. (2012). Decreased levels of nucleotide pyrophosphatase phosphodiesterase 1 are associated with cartilage calcification in osteoarthritis and trigger osteoarthritic changes in mice. *Ann. Rheum. Dis.* **71**, 1249-1253.
Burnstock, G. (2007). Purine and pyrimidine receptors. *Cell. Mol. Life Sci.* **64**, 1471-1483.
Chen, M., Gavrilova, O., Zhao, W.-Q., Nguyen, A., Lorenzo, J., Shen, L., Nackers, L., Pack, S., Jou, W. and Weinstein, L. S. (2005). Increased glucose tolerance and reduced adiposity in the absence of fasting hypoglycemia in mice with liver-specific Gs alpha deficiency. *J. Clin. Invest.* **115**, 3217-3227.
Chuang, P.-T. and McMahon, A. P. (1999). Vertebrate Hedgehog signalling modulated by induction of a Hedgehog-binding protein. *Nature* **397**, 617-621.
Corrales, J. D., Rocco, G. L., Blaess, S., Guo, Q. and Joyner, A. L. (2004). Spatial pattern of sonic hedgehog signaling through Gli genes during cerebellum development. *Development* **131**, 5581-5590.
Di Virgilio, F. (2012). Purines, purinergic receptors, and cancer. *Cancer Res.* **72**, 5441-5447.
Dreier, R. (2010). Hypertrophic differentiation of chondrocytes in osteoarthritis: the developmental aspect of degenerative joint disorders. *Arthritis Res. Ther.* **12**, 216.
Dy, P., Wang, W., Bhattaram, P., Wang, Q., Wang, L., Ballock, R. T. and Lefebvre, V. (2012). Sox9 directs hypertrophic maturation and blocks osteoblast differentiation of growth plate chondrocytes. *Dev. Cell* **22**, 597-609.
Erb, L., Liao, Z., Seye, C. I. and Weisman, G. A. (2006). P2 receptors: intracellular signaling. *Pflugers Arch.* **452**, 552-562.
Gabay, O. and Gabay, C. (2013). Hand osteoarthritis: new insights. *Joint Bone Spine* **80**, 130-134.
Goding, J. W., Grobben, B. and Slegers, H. (2003). Physiological and pathophysiological functions of the ecto-nucleotide pyrophosphatase/phosphodiesterase family. *Biochim. Biophys. Acta* **1638**, 1-19.
Goding, J. W., Terkeltaub, R., Maurice, M., Deterre, P., Sali, A. and Belli, S. I. (1998). Ecto-phosphodiesterase/pyrophosphatase of lymphocytes and non-lymphoid cells: structure and function of the PC-1 family. *Immunol. Rev.* **161**, 11-26.
Goodrich, L. V., Johnson, R. L., Milenkovic, L., McMahon, J. A. and Scott, M. P. (1996). Conservation of the hedgehog/patched signaling pathway from flies to mice: induction of a mouse patched gene by Hedgehog. *Genes Dev.* **10**, 301-312.
Guilak, F. (2011). Biomechanical factors in osteoarthritis. *Best Pract. Res. Clin. Rheumatol.* **25**, 815-823.
Hajjawi, M. O. R., MacRae, V. E., Huesa, C., Boyde, A., Millán, J. L., Arnett, T. R. and Orriss, I. R. (2014). Mineralisation of collagen rich soft tissues and osteocyte lacunae in Enpp1(−/−) mice. *Bone* **69**, 139-147.
Harmey, D., Hessle, L., Narisawa, S., Johnson, K. A., Terkeltaub, R. and Millán, J. L. (2004). Concerted regulation of inorganic pyrophosphate and osteopontin by akp2, enpp1, and ank: an integrated model of the pathogenesis of mineralization disorders. *Am. J. Pathol.* **164**, 1199-1209.
He, X., Zhang, L., Chen, Y., Remke, M., Shih, D., Lu, F., Wang, H., Deng, Y., Yu, Y., Xia, Y. et al. (2014). The G protein alpha subunit Galphas is a tumor suppressor in Sonic hedgehog-driven medulloblastoma. *Nat. Med.* **20**, 1035-1042.
Heinegård, D. and Saxne, T. (2011). The role of the cartilage matrix in osteoarthritis. *Nat. Rev. Rheumatol.* **7**, 50-56.
Ingham, P. W. and McMahon, A. P. (2001). Hedgehog signaling in animal development: paradigms and principles. *Genes Dev.* **15**, 3059-3087.
Jin, Y., Dong, L., Lu, Y., Wu, W., Hao, Q., Zhou, Z., Jiang, J., Zhao, Y. and Zhang, L. (2012). Dimerization and cytoplasmic localization regulate Hippo kinase signaling activity in organ size control. *J. Biol. Chem.* **287**, 5784-5796.
Joeng, K. S. and Long, F. (2009). The Gli2 transcriptional activator is a crucial effector for Ihh signaling in osteoblast development and cartilage vascularization. *Development* **136**, 4177-4185.
Johnson, K., Goding, J., Van Etten, D., Sali, A., Hu, S.-I., Farley, D., Krug, H., Hessle, L., Millán, J. L. and Terkeltaub, R. (2003). Linked deficiencies in extracellular PP(i) and osteopontin mediate pathologic calcification associated with defective PC-1 and ANK expression. *J Bone Miner. Res.* **18**, 994-1004.
Kamekura, S., Kawasaki, Y., Hoshi, K., Shimoaka, T., Chikuda, H., Maruyama, Z., Komori, T., Sato, S., Takeda, S., Karsenty, G. et al. (2006). Contribution of runt-related transcription factor 2 to the pathogenesis of osteoarthritis in mice after induction of knee joint instability. *Arthritis Rheum.* **54**, 2462-2470.
Khakh, B. S. and North, R. A. (2006). P2X receptors as cell-surface ATP sensors in health and disease. *Nature* **442**, 527-532.
Kim, J.-H., Jeon, J., Shin, M., Won, Y., Lee, M., Kwak, J.-S., Lee, G., Rhee, J., Ryu, J.-H., Chun, C.-H. et al. (2014). Regulation of the catabolic cascade in osteoarthritis by the zinc-ZIP8-MTF1 axis. *Cell* **156**, 730-743.
Lecka, J., Ben-David, G., Simhaev, L., Eliahu, S., Oscar, J., Jr, Luyindula, P., Pelletier, J., Fischer, B., Senderowitz, H. and Sevigny, J. (2013). Nonhydrolyzable ATP analogues as selective inhibitors of human NPP1: a combined computational/experimental study. *J. Med. Chem.* **56**, 8308-8320.
Li, Q., Guo, H., Chou, D. W., Berndt, A., Sundberg, J. P. and Uitto, J. (2013). Mutant Enpp1asj mice as a model for generalized arterial calcification of infancy. *Dis. Model Mech.* **6**, 1227-1235.
Lin, A. C., Seeto, B. L., Bartoszko, J. M., Khoury, M. A., Whetstone, H., Ho, L., Hsu, C., Ali, S. A. and Alman, B. A. (2009). Modulating hedgehog signaling can attenuate the severity of osteoarthritis. *Nat. Med.* **15**, 1421-1425.
Long, F., Zhang, X. M., Karp, S., Yang, Y. and McMahon, A. P. (2001). Genetic manipulation of hedgehog signaling in the endochondral skeleton reveals a direct role in the regulation of chondrocyte proliferation. *Development* **128**, 5099-5108.
Lorenz-Depiereux, B., Schnabel, D., Tiosano, D., Häusler, G. and Strom, T. M. (2010). Loss-of-function ENPP1 mutations cause both generalized arterial calcification of infancy and autosomal-recessive hypophosphatemic rickets. *Am. J. Hum. Genet.* **86**, 267-272.
Lories, R. J. and Luyten, F. P. (2011). The bone-cartilage unit in osteoarthritis. *Nat. Rev. Rheumatol.* **7**, 43-49.
Mak, K. K., Chen, M. H., Day, T. F., Chuang, P.-T. and Yang, Y. (2006). Wnt/beta-catenin signaling interacts differentially with Ihh signaling in controlling endochondral bone and synovial joint formation. *Development* **133**, 3695-3707.
Mak, K. K., Bi, Y., Wan, C., Chuang, P.-T., Clemens, T., Young, M. and Yang, Y. (2008a). Hedgehog signaling in mature osteoblasts regulates bone formation and resorption by controlling PTHrP and RANKL expression. *Dev. Cell* **14**, 674-688.
Mak, K. K., Kronenberg, H. M., Chuang, P.-T., Mackem, S. and Yang, Y. (2008b). Indian hedgehog signals independently of PTHrP to promote chondrocyte hypertrophy. *Development* **135**, 1947-1956.
McLeod, M. J. (1980). Differential staining of cartilage and bone in whole mouse fetuses by alcian blue and alizarin red S. *Teratology* **22**, 299-301.
Murshed, M., Harmey, D., Millan, J. L., McKee, M. D. and Karsenty, G. (2005). Unique coexpression in osteoblasts of broadly expressed genes accounts for the spatial restriction of ECM mineralization to bone. *Genes Dev.* **19**, 1093-1104.
Nakashima, K., Zhou, X., Kunkel, G., Zhang, Z., Deng, J. M., Behringer, R. R. and de Crombrugghe, B. (2002). The novel zinc finger-containing transcription factor osterix is required for osteoblast differentiation and bone formation. *Cell* **108**, 17-29.
Neuhold, L. A., Killar, L., Zhao, W., Sung, M.-L. A., Warner, L., Kulik, J., Turner, J., Wu, W., Billinghurst, C., Meijers, T. et al. (2001). Postnatal

expression in hyaline cartilage of constitutively active human collagenase-3 (MMP-13) induces osteoarthritis in mice. *J. Clin. Invest.* **107**, 35-44.
Nitschke, Y. and Rutsch, F. (2012). Generalized arterial calcification of infancy and pseudoxanthoma elasticum: two sides of the same coin. *Front. Genet.* **3**, 302.
Nitschke, Y., Baujat, G., Botschen, U., Wittkampf, T., du Moulin, M., Stella, J., Le Merrer, M., Guest, G., Lambot, K., Tazarourte-Pinturier, M.-F. et al. (2012). Generalized arterial calcification of infancy and pseudoxanthoma elasticum can be caused by mutations in either ENPP1 or ABCC6. *Am. J. Hum. Genet.* **90**, 25-39.
North, R. A. (2002). Molecular physiology of P2X receptors. *Physiol. Rev.* **82**, 1013-1067.
Okawa, A., Ikegawa, S., Nakamura, I., Goto, S., Moriya, H. and Nakamura, Y. (1998). Mapping of a gene responsible for twy (tip-toe walking Yoshimura), a mouse model of ossification of the posterior longitudinal ligament of the spine (OPLL). *Mamm. Genome* **9**, 155-156.
Park, J., Gebhardt, M., Golovchenko, S., Perez-Branguli, F., Hattori, T., Hartmann, C., Zhou, X., deCrombrugghe, B., Stock, M., Schneider, H. et al. (2015). Dual pathways to endochondral osteoblasts: a novel chondrocyte-derived osteoprogenitor cell identified in hypertrophic cartilage. *Biol. Open* **4**, 608-621.
Regard, J. B., Cherman, N., Palmer, D., Kuznetsov, S. A., Celi, F. S., Guettier, J.-M., Chen, M., Bhattacharyya, N., Wess, J., Coughlin, S. R. et al. (2011). Wnt/beta-catenin signaling is differentially regulated by Galpha proteins and contributes to fibrous dysplasia. *Proc. Natl. Acad. Sci. USA* **108**, 20101-20106.
Regard, J. B., Malhotra, D., Gvozdenovic-Jeremic, J., Josey, M., Chen, M., Weinstein, L. S., Lu, J., Shore, E. M., Kaplan, F. S. and Yang, Y. (2013). Activation of Hedgehog signaling by loss of GNAS causes heterotopic ossification. *Nat. Med.* **19**, 1505-1512.
Rodda, S. J. and McMahon, A. P. (2006). Distinct roles for Hedgehog and canonical Wnt signaling in specification, differentiation and maintenance of osteoblast progenitors. *Development* **133**, 3231-3244.
Ruf, N., Uhlenberg, B., Terkeltaub, R., Nürnberg, P. and Rutsch, F. (2005). The mutational spectrum of ENPP1 as arising after the analysis of 23 unrelated patients with generalized arterial calcification of infancy (GACI). *Hum. Mutat.* **25**, 98.
Rutsch, F., Vaingankar, S., Johnson, K., Goldfine, I., Maddux, B., Schauerte, P., Kalhoff, H., Sano, K., Boisvert, W. A., Superti-Furga, A. et al. (2001). PC-1 nucleoside triphosphate pyrophosphohydrolase deficiency in idiopathic infantile arterial calcification. *Am. J. Pathol.* **158**, 543-554.
Rutsch, F., Ruf, N., Vaingankar, S., Toliat, M. R., Suk, A., Höhne, W., Schauer, G., Lehmann, M., Roscioli, T., Schnabel, D. et al. (2003). Mutations in ENPP1 are associated with 'idiopathic' infantile arterial calcification. *Nat. Genet.* **34**, 379-381.
Sellam, J. and Berenbaum, F. (2010). The role of synovitis in pathophysiology and clinical symptoms of osteoarthritis. *Nat. Rev. Rheumatol.* **6**, 625-635.
Serrano, R. L., Yu, W. and Terkeltaub, R. (2014). Mono-allelic and bi-allelic ENPP1 deficiency promote post-injury neointimal hyperplasia associated with increased C/EBP homologous protein expression. *Atherosclerosis* **233**, 493-502.
Spector, T. D. and MacGregor, A. J. (2004). Risk factors for osteoarthritis: genetics. *Osteoarthritis Cartilage* **12** Suppl. A, S39-S44.
Stefan, C., Jansen, S. and Bollen, M. (2005). NPP-type ectophosphodiesterases: unity in diversity. *Trends Biochem. Sci.* **30**, 542-550.
St-Jacques, B., Hammerschmidt, M. and McMahon, A. P. (1999). Indian hedgehog signaling regulates proliferation and differentiation of chondrocytes and is essential for bone formation. *Genes Dev.* **13**, 2072-2086.
Stone, D. M., Hynes, M., Armanini, M., Swanson, T. A., Gu, Q., Johnson, R. L., Scott, M. P., Pennica, D., Goddard, A., Phillips, H. et al. (1996). The tumour-suppressor gene patched encodes a candidate receptor for Sonic hedgehog. *Nature* **384**, 129-134.
Tchetina, E. V. (2011). Developmental mechanisms in articular cartilage degradation in osteoarthritis. *Arthritis* **2011**, 683970.
Topol, L., Jiang, X., Choi, H., Garrett-Beal, L., Carolan, P. J. and Yang, Y. (2003). Wnt-5a inhibits the canonical Wnt pathway by promoting GSK-3-independent beta-catenin degradation. *J. Cell Biol.* **162**, 899-908.
Valdes, A. M., Doherty, M. and Spector, T. D. (2008). The additive effect of individual genes in predicting risk of knee osteoarthritis. *Ann. Rheum. Dis.* **67**, 124-127.
Vortkamp, A., Lee, K., Lanske, B., Segre, G. V., Kronenberg, H. M. and Tabin, C. J. (1996). Regulation of rate of cartilage differentiation by Indian hedgehog and PTH-related protein. *Science* **273**, 613-622.
Wang, F., Flanagan, J., Su, N., Wang, L.-C., Bui, S., Nielson, A., Wu, X., Vo, H.-T., Ma, X.-J. and Luo, Y. (2012). RNAscope: a novel in situ RNA analysis platform for formalin-fixed, paraffin-embedded tissues. *J. Mol. Diagn.* **14**, 22-29.
Yang, G., Zhu, L., Hou, N., Lan, Y., Wu, X.-M., Zhou, B., Teng, Y. and Yang, X. (2014a). Osteogenic fate of hypertrophic chondrocytes. *Cell Res.* **24**, 1266-1269.
Yang, L., Tsang, K. Y., Tang, H. C., Chan, D. and Cheah, K. S. E. (2014b). Hypertrophic chondrocytes can become osteoblasts and osteocytes in endochondral bone formation. *Proc. Natl. Acad. Sci. USA* **111**, 12097-12102.
Zhang, J., Dyment, N. A., Rowe, D. W., Siu, S. Y., Sundberg, J. P., Uitto, J. and Li, Q. (2016). Ectopic mineralization of cartilage and collagen-rich tendons and ligaments in Enpp1asj-2J mice. *Oncotarget* **7**, 12000-12009.
Zhou, X., von der Mark, K., Henry, S., Norton, W., Adams, H. and de Crombrugghe, B. (2014). Chondrocytes transdifferentiate into osteoblasts in endochondral bone during development, postnatal growth and fracture healing in mice. *PLoS Genet.* **10**, e1004820.